COMMUNICATIONS
IN PHYSICS

Volume 32, Number 3 **September 2022**

PAPERS

Communications in Physics, Vol. 32, No. 3 (2022), pp. 295-306
DOI: https://doi.org/10.15625/0868-3166/16748

EXCITONIC SUSCEPTIBILITY FUNCTION IN SEMIMETAL/SEMICONDUCTOR MATERIALS: FORMATION OF THE EXCITONIC CONDENSATE STATE

DO THI HONG HAI† AND NGUYEN THI HAU

Hanoi University of Mining and Geology, Duc Thang, Bac Tu Liem, Hanoi, Vietnam

E-mail: †dothihonghai@humg.edu.vn

Received 22 November 2021; *Accepted for publication 13 April 2022*; *Published 11 May 2022*

Abstract. *The condensate state of excitons in semimetal/semiconductor materials has been considered by analyzing the excitonic susceptibility function in the 2D extended Falicov-Kimball model including the electron-phonon interaction. The excitonic susceptibility in the system has been calculated by using the Hartree-Fock approximation. From numerical results, we have set up the phase diagrams of the excitonic condensate state. The phase diagrams confirm that the electron-phonon coupling plays an important role as well as the Coulomb attraction does in establishing the excitonic condensed phase at low temperature. The condensate phase of excitons is found within a limited range of the Coulomb attraction as the electron-phonon coupling is large enough. Depending on the electron-phonon coupling and the Coulomb attraction, the BCS-BEC crossover of the excitonic condensation phase has also been pointed out.*

Keywords: excitonic condensation; extended Falicov-Kimball model; electron-phonon coupling; excitonic susceptibility.

Classification numbers: 71.35.-y.

I. INTRODUCTION

Excitons in solids are formed by the Coulomb attraction between electrons in the conduction band and holes in the valence band. In semimetal materials with narrow band-overlap or in semiconductor materials which have small band-gap, a new macroscopic quantum state of these excitons can be established if the temperature is sufficiently low [1]. It is called the excitonic insulator (EI) state which was theoretically proposed almost 60 years ago [2–4]. Ones believe that the semimetal (SM)-EI transition is similar to the superconductivity theory of Bardeen-Cooper-Schrieffer (BCS), while the semiconductor (SC)-EI transition is considered as a Bose-Einstein condensation (BEC) of preformed tightly bound excitons. Therefore, when studying the EI phase,

one often also discusses the BCS-BEC crossover of this state. The EI phase also has been expected to have many unusual properties, such as crystallized excitonium, superfluidity and excitonic high-temperature superconductivity. This state, therefore, has attracted interest of condensed matter physicists and material scientists.

Although being theoretically predicted very early, the EI state is rare because excitons have a short lifetime, so it is difficult to be observed experimentally. However, in recent years, there have been a lot of experimental observations on some materials that affirm the existence of the EI phase. For instance, in the pressure-sensitive mixed valence material $TmSe_{0.45}Te_{0.55}$, experimental results of electrical and thermal transport properties have indicated a stabilized excitonic condensation state at low temperature in the limited range of the pressure from 5 kbar to 13 kbar [5–7]. When the pressure is larger than 13kbar, the system transfers into the SM state (the energy gap $E_g \leq 0$), while the pressure is less than 5kbar, the system is in the SC state ($E_g > 0$). By using the momentum-resolved electron energy-loss spectroscopy, an evidence for the excitonic condensation has been shown in the transition metal dichalcogenide semimetal $1T$-$TiSe_2$ [8]. Another EI candidate is the small gap quasi-onedimensional chalcogenide Ta_2NiSe_5. Indeed, experimental results in this material have confirmed the existence of the EI state, for example, the optical conductivity [9, 10] or phonon properties of the material [11, 12].

Normally, when studying the EI state in the exciton systems, it is common to use the pure electronic models [13–16]. Most notably, the extended Falicov-Kimball model (EFKM) with narrow $f-$band and wide $c-$band including the Coulomb attraction between electrons in the conduction band and holes in the valence band closely matches the situation in the intermediate-valence compounds. This model has been considered as a simple model to investigate the EI state by lots of numerical and theoretical methods. However, when using this model, the interaction between electrons and phonons is completely ignored. Whereas this coupling must be studied meticulously in driving the condensation of excitons in the SM and SC materials. Indeed, experimental observations reveal that the phonon plays an important role in the establishment of the excitonic condensation state in transition metal dichalcoginides [8, 17]. Besides, in $TmSe_{0.45}Te_{0.55}$, ones believe that phonons assist $4f$ holes in pairing with $5d$ electrons to create excitons [5, 18]. Therefore, in this paper, we investigate effects of both the electron-phonon interaction and the Coulomb attraction on the formation of the EI phase in SM/SC materials at low temperature.

We have studied the excitonic condensation phase in the EFKM involving electron-phonon interaction via investigating the properties of the condensate order parameter in some recent works [19, 20]. We have constructed the EI phase diagrams including the BCS-BEC crossover in the systems due to the influence of temperature, the Coulomb attraction as well as the electron-phonon coupling. However, the order parameter investigation reveals only the properties of the condensation at temperature below the critical temperature. On the other hand, recent studies of Ta_2NiSe_5 give us different views than the initial assumptions about the condensation formation of excitons [21, 22]. It is necessary, therefore, to consider the excitonic susceptibility function to clearly describe the condensation mechanism of the exciton systems above the transition temperature.

In the present work, we set up and discuss the phase diagrams of the EI state including the BCS-BEC crossover in SM/SC materials in the framework of the 2D EFKM with the presence of the electron-phonon interaction through investigating the properties of the excitonic susceptibility function. Applying the Hartree-Fock approximation (HFA), we obtained a set of self-consistent

equations to determine the excitonic susceptibility function. The EI phase diagrams in the system are constructed through analyzing the divergence signature of the static excitonic susceptibility function from numerical results.

This paper is organized as follows. We introduce the 2D EFKM involving electron-phonon interaction for SM/SC materials in section II. Then, applying the Hartree-Fock approximation to the model to determine the excitonic susceptibility function is presented in section III. In section IV, we establish and discuss phase diagrams of the EI state from the numerical results. In the final section, the conclusion is given.

II. MODEL

In the momentum space, the EFKM involving the electron-phonon interaction is written by the following Hamiltonian

$$\mathscr{H} = \mathscr{H}_e + \mathscr{H}_{ph} + \mathscr{H}_{e-e} + \mathscr{H}_{e-ph}, \tag{1}$$

where $\mathscr{H}_e$ and $\mathscr{H}_{ph}$ are the non-interacting parts of the electron and phonon systems, respectively. $\mathscr{H}_e$ describes f electrons in the valence band and c electrons in the conduction band

$$\mathscr{H}_e = \sum_{\mathbf{k}} \varepsilon^f_{\mathbf{k}} f^\dagger_{\mathbf{k}} f_{\mathbf{k}} + \sum_{\mathbf{k}} \varepsilon^c_{\mathbf{k}} c^\dagger_{\mathbf{k}} c_{\mathbf{k}}, \tag{2}$$

with $f_{\mathbf{k}}(f^\dagger_{\mathbf{k}})$ and $c_{\mathbf{k}}(c^\dagger_{\mathbf{k}})$ are annihilation (creation) operators of f electrons and c electrons carrying momentum $\mathbf{k}$, respectively. The dispersion energy of $c(f)$ electron is written in a form

$$\varepsilon^{c(f)}_{\mathbf{k}} = \varepsilon^{c(f)} - t^{c(f)}\gamma_{\mathbf{k}} - \mu, \tag{3}$$

where $\varepsilon^{c(f)}$ is the on-site energy of the $c(f)$ electron; $t^{c(f)}$ is the nearest-neighbor particle transfer amplitude; $\gamma_{\mathbf{k}} = 2(\cos k_x + \cos k_y)$ indicates the nearest-neighbor hopping in the 2D systems, and μ is the chemical potential. The free phonon part in the systems with phonon annihilation (creation) operator $b_{\mathbf{q}}(b^\dagger_{\mathbf{q}})$ carrying momentum $\mathbf{q}$ is described by

$$\mathscr{H}_{ph} = \omega_0 \sum_{\mathbf{q}} b^\dagger_{\mathbf{q}} b_{\mathbf{q}}, \tag{4}$$

where ω_0 is dispersionless single mode phonon energy. Here, we consider only the optical phonon which is described by the Einstein model where the phonon frequency ω_0 does not depend on momentum. This is completely consistent with the situation of the phonon systems in some materials that are candidates to observe the excitonic condensation at low temperature [7, 23–25]. For instance, in $TmSe_{0.45}Te_{0.55}$, the density of optical phonons decreases linearly when the temperature decreases. This might be due to the binding of optical phonons to electrons when the temperature is lower than the transition temperature [7]. Or from the experimental data of X-ray thermal diffraction measurement in transition-metal dichalcogenide $TiSe_2$, the existence of optical phonons has also been confirmed in the excitonic condensate state at a sufficiently low temperature [23, 24]. Most recently, the results of Raman spectroscopy in direct gap semimetal Ta_2NiSe_5 have confirmed a strong electron–optical phonon coupling that mediates to form the excitonic condensation state a low temperature [25].

The last two terms in Eq. (1), $\mathscr{H}_{e-e}$ and $\mathscr{H}_{e-ph}$, which describe the Coulomb interaction part between $c-f$ electrons and the electron-phonon interaction part, respectively, read

$$\mathscr{H}_{e-e} = \frac{U}{N}\sum_{\mathbf{k},\mathbf{k}',\mathbf{q}} c^{\dagger}_{\mathbf{k}+\mathbf{q}} c_{\mathbf{k}'} f^{\dagger}_{\mathbf{k}'-\mathbf{q}} f_{\mathbf{k}}, \tag{5}$$

$$\mathscr{H}_{e-ph} = \frac{g}{\sqrt{N}}\sum_{\mathbf{kq}}\left[c^{\dagger}_{\mathbf{k}+\mathbf{q}} f_{\mathbf{k}}\left(b^{\dagger}_{-\mathbf{q}} + b_{\mathbf{q}}\right) + \text{H.c.}\right], \tag{6}$$

with U is the Coulomb attraction intensity; g is the electron-phonon coupling constant and N is the number of unit cells. In the present investigation, we consider only the optical phonon where the phonon frequency ω_0 is a constant, so the electron-phonon coupling g also does not depend on the wave vector. In principle, Coulomb interactions between $c-c$ and $f-f$ electrons might have been taken into account, but we neglect them because they cause only simple shifts in the one-particle electronic dispersions.

In the present work, we assume that a $c-f$ electron bounding state is equivalent to an exciton state and analyze the excitonic susceptibility creating an exciton excitation with momentum $\mathbf{q}$ in the system. In the next section, the excitonic susceptibility function is calculated by using the HFA.

III. THE HARTREE-FOCK APPROXIMATION

In general, it is difficult to exactly solve the Hamiltonian in Eq. (1) because of a many-body problem. In our study, by applying the HFA, the problem reduces to a single-particle problem and then the HFA Hamiltonian is written as

$$\mathscr{H}^{HF} = \mathscr{H}^{HF}_{ph} + \mathscr{H}^{HF}_{e}, \tag{7}$$

where the phononic part is given by

$$\mathscr{H}^{HF}_{ph} = \omega_0\sum_{\mathbf{q}} b^{\dagger}_{\mathbf{q}} b_{\mathbf{q}} + \sqrt{N}h(b^{\dagger}_{-\mathbf{q}} + b_{-\mathbf{q}}), \tag{8}$$

and the electronic part reads

$$\mathscr{H}^{HF}_{e} = \sum_{\mathbf{k}} \overline{\varepsilon}^{f}_{\mathbf{k}} f^{\dagger}_{\mathbf{k}} f_{\mathbf{k}} + \sum_{\mathbf{k}} \overline{\varepsilon}^{c}_{\mathbf{k}} c^{\dagger}_{\mathbf{k}} c_{\mathbf{k}} + \Lambda\sum_{\mathbf{k}} (c^{\dagger}_{\mathbf{k}+\mathbf{q}} f_{\mathbf{k}} + f^{\dagger}_{\mathbf{k}} c_{\mathbf{k}+\mathbf{q}}).$$

Here because of the Hartree shifts, the electronic excitation energies are rewritten as

$$\overline{\varepsilon}^{c(f)}_{\mathbf{k}} = \varepsilon^{c(f)}_{\mathbf{k}} + U n^{f(c)}, \tag{9}$$

where

$$n^{c} = \frac{1}{N}\sum_{\mathbf{k}} \langle c^{\dagger}_{\mathbf{k}} c_{\mathbf{k}}\rangle, \qquad n^{f} = \frac{1}{N}\sum_{\mathbf{k}} \langle f^{\dagger}_{\mathbf{k}} f_{\mathbf{k}}\rangle, \tag{10}$$

are the c electrons density and f electrons density, respectively, with

$$\langle c^{\dagger}_{\mathbf{k}} c_{\mathbf{k}}\rangle = \langle n^{c}_{\mathbf{k}}\rangle = \frac{1}{1+e^{\beta\overline{\varepsilon}^{c}_{\mathbf{k}}}} = n_F(\overline{\varepsilon}^{f}_{\mathbf{k}}), \tag{11}$$

$$\langle f^{\dagger}_{\mathbf{k}} f_{\mathbf{k}}\rangle = \langle n^{f}_{\mathbf{k}}\rangle = \frac{1}{1+e^{\beta\overline{\varepsilon}^{f}_{\mathbf{k}}}} = n_F(\overline{\varepsilon}^{f}_{\mathbf{k}}), \tag{12}$$

where $n_F(\epsilon)$ is the Fermi-Dirac distribution function and $\beta = 1/T$.

In Eqs. (8) and (9), h and Λ are the additional fields, given by

$$h = \frac{g}{N}\sum_{\mathbf{k}}(\Lambda_{\mathbf{k}}+\Lambda^*_{\mathbf{k}}), \tag{13}$$

$$\Lambda = \frac{g}{\sqrt{N}}\langle b^\dagger_{-\mathbf{q}}+b_{-\mathbf{q}}\rangle - \frac{U}{N}\sum_{\mathbf{k}}\Lambda_{\mathbf{k}}, \tag{14}$$

which contain the term representing the hybridization of the c-electron and the f-electron, $\Lambda_{\mathbf{k}} = \langle c^\dagger_{\mathbf{k}+\mathbf{q}} f_{\mathbf{k}}\rangle$. It therefore is considered to be the excitonic condensed state order parameter. Diagonalizing the HFA Hamiltonian in Eq.(7) by using the Bogoliubov transformation, we find the expectation value

$$\Lambda_{\mathbf{k}} = -[n_F(E^1_{\mathbf{k}}) - n_F(E^2_{\mathbf{k}})]\mathrm{sgn}(\overline{\varepsilon}^f_{\mathbf{k}} - \overline{\varepsilon}^c_{\mathbf{k}+\mathbf{q}})\frac{\Lambda}{\Gamma_{\mathbf{k}}}, \tag{15}$$

here

$$E^{1(2)}_{\mathbf{k}} = \frac{\overline{\varepsilon}^f_{\mathbf{k}}+\overline{\varepsilon}^c_{\mathbf{k}+\mathbf{q}}}{2} \mp \frac{\mathrm{sgn}(\overline{\varepsilon}^f_{\mathbf{k}} - \overline{\varepsilon}^c_{\mathbf{k}+\mathbf{q}})}{2}\Gamma_{\mathbf{k}}, \tag{16}$$

and

$$\Gamma_{\mathbf{k}} = \sqrt{(\overline{\varepsilon}^c_{\mathbf{k}+\mathbf{q}} - \overline{\varepsilon}^f_{\mathbf{k}})^2 + 4|\Lambda|^2}. \tag{17}$$

In the previous studies, we addressed the EI phase diagrams including the BCS-BEC crossover in the exciton systems via investigating the properties of the order parameter [19, 20, 26]. In this paper, we analyze the excitonic susceptibility creating a bound state of electron-hole pair carrying momentum $\mathbf{q}$ in the system. The excitonic susceptibility function in momentum space is defined

$$\chi(\mathbf{q},\omega) = -\frac{1}{N}\sum_{\mathbf{k}\mathbf{k}'}\langle\langle f^\dagger_{\mathbf{k}} c_{\mathbf{k}+\mathbf{q}} | c^\dagger_{\mathbf{k}'+\mathbf{q}} f_{\mathbf{k}'}\rangle\rangle_\omega. \tag{18}$$

Using Hamiltonian (1) and writing the equation of motion for two-particle Green's function, we obtain

$$\begin{aligned}\omega\langle\langle f^\dagger_{\mathbf{k}} c_{\mathbf{k}+\mathbf{q}} | c^\dagger_{\mathbf{k}'+\mathbf{q}} f_{\mathbf{k}'}\rangle\rangle_\omega &= \langle n^f_{\mathbf{k}}\rangle - \langle n^c_{\mathbf{k}+\mathbf{q}}\rangle + (\varepsilon^c_{\mathbf{k}+\mathbf{q}} - \varepsilon^f_{\mathbf{k}})\langle\langle f^\dagger_{\mathbf{k}} c_{\mathbf{k}+\mathbf{q}} | c^\dagger_{\mathbf{k}'+\mathbf{q}} f_{\mathbf{k}'}\rangle\rangle_\omega \\ &+\frac{U}{N}\sum_{\mathbf{k}''\mathbf{q}_1}(\langle\langle f^\dagger_{\mathbf{k}} c_{\mathbf{k}''} f^\dagger_{\mathbf{k}''-\mathbf{q}_1} f_{\mathbf{k}+\mathbf{q}-\mathbf{q}_1} | c^\dagger_{\mathbf{k}'+\mathbf{q}} f_{\mathbf{k}'}\rangle\rangle_\omega - \langle\langle c^\dagger_{\mathbf{k}+\mathbf{q}_1} c_{\mathbf{k}''} f^\dagger_{\mathbf{k}''-\mathbf{q}_1} c_{\mathbf{k}+\mathbf{q}} | c^\dagger_{\mathbf{k}'+\mathbf{q}} f_{\mathbf{k}'}\rangle\rangle_\omega) \\ &+\frac{g}{\sqrt{N}}\sum_{\mathbf{q}_1}(\langle\langle f^\dagger_{\mathbf{k}} f_{\mathbf{k}+\mathbf{q}-\mathbf{q}_1}(b^\dagger_{-\mathbf{q}_1}+b_{\mathbf{q}_1}) | c^\dagger_{\mathbf{k}'+\mathbf{q}} f_{\mathbf{k}'}\rangle\rangle_\omega - \langle\langle c^\dagger_{\mathbf{k}+\mathbf{q}_1} c_{\mathbf{k}+\mathbf{q}}(b^\dagger_{-\mathbf{q}_1}+b_{\mathbf{q}_1}) | c^\dagger_{\mathbf{k}'+\mathbf{q}} f_{\mathbf{k}'}\rangle\rangle_\omega).\end{aligned} \tag{19}$$

According to the principles of random phase approximation, the additional operators in the higher order Green's functions are replaced by their averages

$$\begin{aligned}&\sum_{\mathbf{k}''\mathbf{q}_1}\langle\langle f^\dagger_{\mathbf{k}} c_{\mathbf{k}''} f^\dagger_{\mathbf{k}''-\mathbf{q}_1} f_{\mathbf{k}+\mathbf{q}-\mathbf{q}_1} | c^\dagger_{\mathbf{k}'+\mathbf{q}} f_{\mathbf{k}'}\rangle\rangle_\omega \\ &\qquad\approx \sum_{\mathbf{q}_1}\langle n^f_{\mathbf{k}+\mathbf{q}-\mathbf{q}_1}\rangle\langle\langle f^\dagger_{\mathbf{k}} c_{\mathbf{k}+\mathbf{q}} | c^\dagger_{\mathbf{k}'+\mathbf{q}} f_{\mathbf{k}'}\rangle\rangle_\omega - \sum_{\mathbf{k}_2}\langle n^f_{\mathbf{k}}\rangle\langle\langle f^\dagger_{\mathbf{k}_2} c_{\mathbf{k}_2+\mathbf{q}} | c^\dagger_{\mathbf{k}'+\mathbf{q}} f_{\mathbf{k}'}\rangle\rangle_\omega,\end{aligned} \tag{20}$$

$$\sum_{\mathbf{k}''\mathbf{q_1}} \langle\langle c^\dagger_{\mathbf{k}+\mathbf{q_1}} c_{\mathbf{k}''} f^\dagger_{\mathbf{k}''-\mathbf{q_1}} c_{\mathbf{k}+\mathbf{q}} | c^\dagger_{\mathbf{k}'+\mathbf{q}} f_{\mathbf{k}'} \rangle\rangle_\omega$$
$$\approx \sum_{\mathbf{q_1}} \langle n^c_{\mathbf{k}+\mathbf{q_1}} \rangle \langle\langle f^\dagger_{\mathbf{k}} c_{\mathbf{k}+\mathbf{q}} | c^\dagger_{\mathbf{k}'+\mathbf{q}} f_{\mathbf{k}'} \rangle\rangle_\omega - \sum_{\mathbf{k_2}} \langle n^c_{\mathbf{k}+\mathbf{q}} \rangle \langle\langle f^\dagger_{\mathbf{k_2}} c_{\mathbf{k_2}+\mathbf{q}} | c^\dagger_{\mathbf{k}'+\mathbf{q}} f_{\mathbf{k}'} \rangle\rangle_\omega, \quad (21)$$

and

$$\langle\langle \sum_{\mathbf{q_1}} f^\dagger_{\mathbf{k}} f_{\mathbf{k}+\mathbf{q}-\mathbf{q_1}} (b^\dagger_{-\mathbf{q_1}} + b_{\mathbf{q_1}}) | c^\dagger_{\mathbf{k}'+\mathbf{q}} f_{\mathbf{k}'} \rangle\rangle_\omega \approx \langle n^f_{\mathbf{k}} \rangle \langle\langle (b^\dagger_{-\mathbf{q}} + b_{\mathbf{q}}) | c^\dagger_{\mathbf{k}'+\mathbf{q}} f_{\mathbf{k}'} \rangle\rangle_\omega, \quad (22)$$

$$\langle\langle \sum_{\mathbf{q_1}} c^\dagger_{\mathbf{k}+\mathbf{q_1}} c_{\mathbf{k}+\mathbf{q}} (b^\dagger_{-\mathbf{q_1}} + b_{\mathbf{q_1}}) | c^\dagger_{\mathbf{k}'+\mathbf{q}} f_{\mathbf{k}'} \rangle\rangle_\omega \approx \langle n^c_{\mathbf{k}+\mathbf{q}} \rangle \langle\langle (b^\dagger_{-\mathbf{q}} + b_{\mathbf{q}}) | c^\dagger_{\mathbf{k}'+\mathbf{q}} f_{\mathbf{k}'} \rangle\rangle_\omega. \quad (23)$$

Writing the equation of motion for $\langle\langle (b^\dagger_{-\mathbf{q}} + b_{\mathbf{q}}) | c^\dagger_{\mathbf{k}'+\mathbf{q}} f_{\mathbf{k}'} \rangle\rangle_\omega$ and setting

$$\omega^{cf}_{\mathbf{k}}(\mathbf{q}) = \overline{\varepsilon}^c_{\mathbf{k}+\mathbf{q}} - \overline{\varepsilon}^f_{\mathbf{k}}, \quad (24)$$

and

$$\chi^{0b}(\mathbf{q},\omega) = \frac{1}{N} \sum_{\mathbf{k}} \frac{\langle n^c_{\mathbf{k}-\mathbf{q}} \rangle - \langle n^f_{\mathbf{k}} \rangle}{\omega - \omega^0_{\mathbf{k}}(\mathbf{q})}, \quad (25)$$

with $\omega^0_{\mathbf{k}}(\mathbf{q}) = \overline{\varepsilon}^f_{\mathbf{k}} - \overline{\varepsilon}^c_{\mathbf{k}-\mathbf{q}}$, we get

$$[\omega - \omega^{cf}_{\mathbf{k}}(\mathbf{q})] \langle\langle f^\dagger_{\mathbf{k}} c_{\mathbf{k}+\mathbf{q}} | c^\dagger_{\mathbf{k}'+\mathbf{q}} f_{\mathbf{k}'} \rangle\rangle_\omega = \langle n^f_{\mathbf{k}} \rangle - \langle n^c_{\mathbf{k}+\mathbf{q}} \rangle - (\langle n^f_{\mathbf{k}} \rangle - \langle n^c_{\mathbf{k}+\mathbf{q}} \rangle) \frac{U}{N} \sum_{\mathbf{k_2}} \langle\langle f^\dagger_{\mathbf{k_2}} c_{\mathbf{k_2}+\mathbf{q}} | c^\dagger_{\mathbf{k}'+\mathbf{q}} f_{\mathbf{k}'} \rangle\rangle_\omega$$
$$+ \frac{2g^2\omega_0}{N} \frac{\langle n^f_{\mathbf{k}} \rangle - \langle n^c_{\mathbf{k}+\mathbf{q}} \rangle}{\omega^2 - \omega_0^2 - \frac{2g^2\omega_0 \chi^{0b}(\mathbf{q},\omega)}{1+U\chi^{0b}(\mathbf{q},\omega)}} \sum_{\mathbf{k_1}} \langle\langle f^\dagger_{\mathbf{k_1}} c_{\mathbf{k_1}+\mathbf{q}} | c^\dagger_{\mathbf{k}'+\mathbf{q}} f_{\mathbf{k}'} \rangle\rangle_\omega, \quad (26)$$

Finally, we sum over $\mathbf{k}$ Eq. (26) and rename summation indices, the excitonic susceptibility can be written as

$$\chi(\mathbf{q},\omega) = \frac{-\chi^0(\mathbf{q},\omega)}{1 + U\chi^0(\mathbf{q},\omega) - \frac{2g^2\omega_0\chi^0(\mathbf{q},\omega)}{\omega^2 - \omega_0^2 - \frac{2g^2\omega_0\chi^{0b}(\mathbf{q},\omega)}{1+U\chi^{0b}(\mathbf{q},\omega)}}}, \quad (27)$$

where

$$\chi^0(\mathbf{q},\omega) = \frac{1}{N} \sum_{\mathbf{k}} \frac{\langle n^f_{\mathbf{k}} \rangle - \langle n^c_{\mathbf{k}+\mathbf{q}} \rangle}{\omega - \omega^{cf}_{\mathbf{k}}(\mathbf{q})}, \quad (28)$$

here $\langle n^f_{\mathbf{k}} \rangle$ and $\langle n^c_{\mathbf{k}+\mathbf{q}} \rangle$ are determined from Eqs. (11) and (12).

In order to construct phase diagrams of the EI state, in our work, the static excitonic susceptibility function $\chi(\mathbf{q},\omega)$ for $\omega \to 0$ is computed. We also focus on excitons carrying momentum $\mathbf{q} = \mathbf{0}$ which is consistent with excitons in Ta_2NiSe_5 [27]. The excitonic susceptibility function exhibits excitons fluctuation so the existence of the EI state in the system is indicated by its divergence. We, therefore, focus on the condition for the divergence of the static excitonic susceptibility function $\chi = \chi(\mathbf{0},\mathbf{0})$ to establish phase diagrams of the excitonic condensate state including the BCS-BEC crossover.

IV. NUMERICAL RESULTS AND DISCUSSION

To understand in detail the excitonic condensed phase transition in SM and SC materials, we display and discuss the phase diagrams which are constructed from numerical results of analytical calculation results in the previous section. Without loss of generality, for a 2D system containing $N = 500 \times 500$ lattice sites, the expected values are obtained by solving the above set of self-consistent equations [Eqs. (9-17)] with using $t^c = 1$ as the unit of energy. Then, the static excitonic susceptibility function χ is determined from Eq. (27). We also choose $t^f = 0.3$; $\varepsilon^c - \varepsilon^f = 2.0$ and $\omega_0 = 2.0$. In this case, all quantities are evaluated in units of t^c. For given parameters, the self-consistent calculation obtains a solution if the relative error of all quantities is less than 10^{-12}.

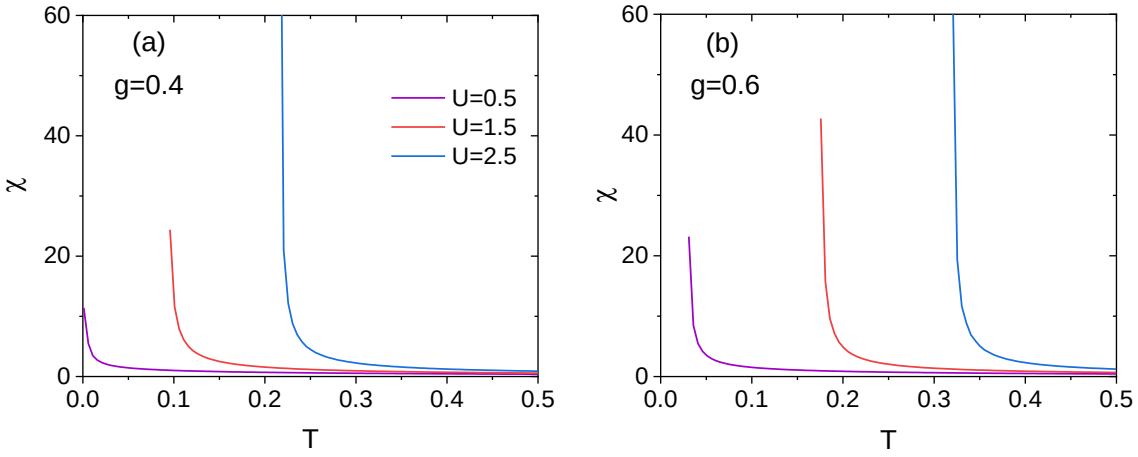

Fig. 1. The static excitonic susceptibility χ depends on temperature T for some values of the Coulomb attraction U in the weak interaction regime at $g = 0.4$ (a) and $g = 0.6$ (b).

Firstly, we present the dependence of the static excitonic susceptibility function χ on temperature T for various values of the Coulomb attraction U in the weak interaction regime and two values of the electron-phonon coupling $g = 0.4$ and $g = 0.6$. Fig. 1 indicates that the condensate phase of excitons stabilizes at sufficiently low temperature. Indeed, for a given Coulomb attraction, the static excitonic susceptibility function χ increases as decreasing the temperature. In particular, in low temperature regime, the static excitonic susceptibility function increases strongly and then diverges as the temperature drops to a critical value T_c. This critical value of the temperature is called an excitonic condensate state transition temperature. When the temperature is low enough, $T \leq T_c$, the system settles in the EI state. In the high temperature regime, the large thermal energy destroys a part of the $c-f$ electron bounding state leading to weakening the EI state, which is illustrated by a decrease of χ. If the temperature is higher than the critical temperature, $T > T_c$, all the excitonic binding states are broken and the system transfers to the electron-hole plasma state. Fig. 1 also shows that in the weak Coulomb interaction region, the critical temperature T_c increases as enlarging the Coulomb interaction U. Comparing Fig. 1a and Fig. 1b we also find that T_c increases as growing the electron-phonon coupling g. This suggests an important role of the electron-phonon coupling in the formation of the EI state. In our previous studies, the role of both the phonons and the Coulomb attraction in formation and condensation of the electron-hole

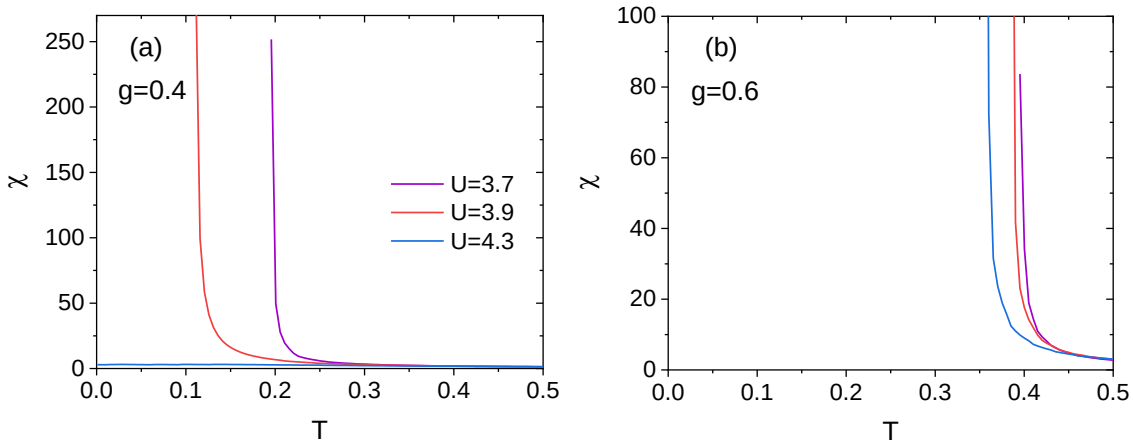

Fig. 2. The static excitonic susceptibility χ depends on the temperature T for some values of the Coulomb attraction U in the strong interaction regime at $g = 0.4$ (a) and $g = 0.6$ (b).

pairs and excitons has been affirmed [19, 20]. In this case, we also see that when a given electron–phonon coupling constant is great enough, $g = 0.6$, in an assistance of phonons, excitons in the system condense at the critical value U_{c1} is relatively small, $U_{c1} < 0.5$ (see Fig. 1b).

Fig. 2 displays the temperature T dependence of the static excitonic susceptibility function χ for some values of the Coulomb attraction U in the strong interaction regime with the same parameter sets as Fig. 1. Similar to Fig. 1, Fig. 2 still shows the divergence property of the static excitonic susceptibility function χ as decreasing the temperature. However, contrary to Fig. 1, Fig. 2 shows that T_c decreases as raising U in the strong interaction regime. This means that the EI phase is found only in a finite range of the Coulomb attraction, from U_{c1} to U_{c2}. Indeed, for $U < U_{c1}$, the Coulomb attraction is not strong enough to pair c electrons and f electrons forming excitons, the system therefore exists in the SM state with overlapping c- and f-bands. Increasing U to a sufficiently large value to cause the electronic hybridization, excitons therefore can be formed and condense. However, increasing U also grows a separation of the c band from f band. It thereby reduces the possibility of $c-f$ electrons pairing to form exciton if U is greater than U_{c2}, for instance, in Fig. 2a, $U \geq 4.3$. Then, the value of the static excitonic susceptibility function χ is insignificant and the system settles in the SC phase. We therefore confirm that the system stabilizes in the EI phase once the Coulomb attraction is above the lower critical value U_{c1} and below the upper critical value U_{c2}. These diagrams also indicate that, increasing electron-phonon coupling, both two critical values U_{c2} and T_c increase. The results obtained here are in a complete agreement with the results in our previous studies based on considering the EI state order parameters [19, 20] as well as studies in purely electronic models [14, 15, 28, 29].

In order to describe in detail effects of the Coulomb attraction on the condensed state nature of the excitons in the system, we display in Fig. 3 the dependence of the EI order parameter $\Lambda_{\mathbf{k}}$ on the momentum and the Coulomb interaction at $g = 0.6$. The diagram confirms that the EI phase is only established as the value of the Coulomb attraction is in a limited range $U_{c1} \leq U \leq U_{c2}$. When increasing U to a sufficiently large value, from U_{c1} to U_{c2}, the energy gap due to the electron-hole

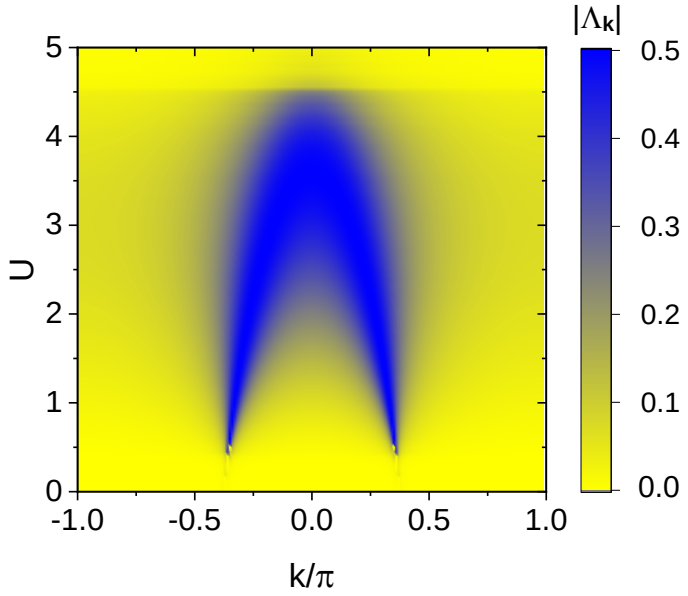

Fig. 3. The momentum $\mathbf{k}$ and the Coulomb interaction U dependence of the EI order parameter $\Lambda_{\mathbf{k}}$ in the first Brillouin zone for $g = 0.6$.

hybridization opens, then the system settles in the EI phase. In the weak interaction regime, the two energy bands overlap strongly leading to a large Fermi surface, the hybridization of the electrons and holes near the Fermi surface is built up and the EI phase is formed by the condensation of electron-hole pairs in a BCS-type. In this case, the EI order parameter $\Lambda_{\mathbf{k}}$ peaks at momentum $\mathbf{k}$ next to the Fermi momentum because only the electrons and holes near the Fermi surface form the excitons. In contrast, in the strong interaction regime, although the $c-f$ bands are separated, a sufficiently large Coulomb attraction will amplify the binding between electrons and holes to form tightly bound excitons. Accordingly, the Fermi surface shrinks into a point, then a large amount of excitons are formed and condense in the BEC-type with the peak of the EI order parameter $\Lambda_{\mathbf{k}}$ is at momentum $\mathbf{k} = \mathbf{0}$. We therefore propose the phase boundary of the EI state between the weak interaction regime and the strong interaction regime is obtained from these positions.

Finally, we display the phase diagrams in the (U,g) plane of the model for two values of the temperature at $g = 0.6$. Our phase diagrams are obtained by investigating the divergence of the static excitonic susceptibility function χ. For a given temperature T, we still see that there are the lower limit value U_{c1} and the upper one U_{c2} of the Coulomb attraction for the EI state even without electron-phonon coupling, $g = 0$. For example, at $T = 0$ and $g = 0$, the obtained values are $(U_{c1}, U_{c2}) = (0.88, 3.53)$ (see Fig. 4a). When the electron-phonon coupling increases, U_{c1} decreases and U_{c2} increases leading to an expansion of the EI phase region. This means that the stronger electron-phonon coupling is, the higher ability of $c-f$ electrons pairing to form exciton is. The role of phonons has also been confirmed to induce the orthorhombic-monoclinic structural phase transition when the SM-EI transition takes place [30, 31]. At $U < U_{c1}$ and the electron-phonon coupling constant is smaller than a critical value, excitonic bound states cannot be formed

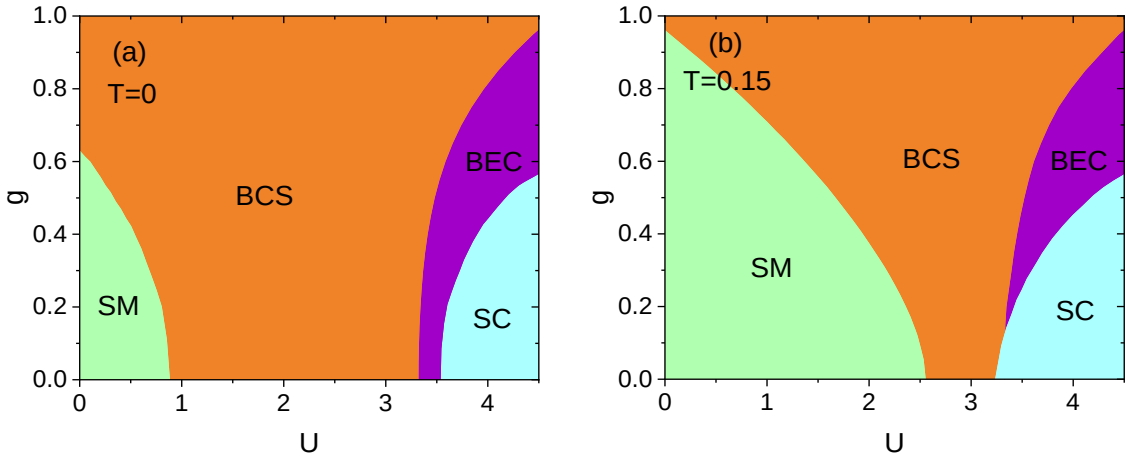

Fig. 4. Phase diagrams of the EI state of the EFKM involving the electron-phonon interaction in the (U, g) plane for two values of T. The EI phase in BCS/BEC-type is indicated by orange/violet region and the SM/SC phase is pointed out by the green/blue region, respectively.

because of the weak interaction, so the system is in the SM phase. If the Coulomb attraction intensity increases from U_{c1} to U_{c2}, the energy gap due to the electron-hole hybridization opens, then the system settles in the EI phase. In the weak Coulomb attraction regime, the hybridization of the electrons and holes near the Fermi surface is built up and the EI typifies the BCS-type. In contrast, increasing the Coulomb attraction to the strong interaction regime, the Coulomb attraction is sufficiently great to bind electron-hole forming tightly bound exciton. The BEC-type condensation of these excitons is formed. If the Coulomb attraction is so strong that it is greater than U_{c2}, because of the contribution of the Coulomb attraction to the Hartree term, the c-bands and the f-bands are split. That prevents the pairing of c electrons and f electrons, the excitonic condensation state therefore is destroyed and the system transfers to the SC phase. Growing the temperature T, the critical value of the electron-phonon coupling constant also increases which leads to a decrease in the EI phase window. These phase diagrams once again confirm the role of both the electron-phonon coupling and the Coulomb interaction in formation and condensation of excitons. Our results fit quite well with the experimental observation of P. Wachter in rare-earth chalcogenide $TmSe_{0.45}Te_{0.55}$ [7, 32]. At sufficiently large external pressure, $4f$- and $5d$-bands overlap, in an assistance of phonons, then excitons can be formed and drop into the EI state once the temperature is low enough. These phase diagrams are similar to the ones given in Ref. [19,33]. But in this work, we present in detail effects of the temperature on the excitonic phase structure in the system. Increasing T to $T = 0.15$ in Fig.4b, leads to both the condensed regions of excitons in the BCS-type and the BEC-type are shrunk, and the SM/SC region is expanded. If the temperature is raised to a value higher than the critical temperature T_c, all binding states are broken and the system transfers to a plasma state of electrons and holes. These phase diagrams agree qualitatively with our phase diagrams obtained which are based on investigating the properties of the condensate order parameters [19]. This confirms the reliability of our study method and results.

V. CONCLUSION

In this paper, by calculating the excitonic susceptibility function, we have considered the formation and condensation of excitons in SM/SC materials via the 2D EFKM involving the electron-phonon interaction. We have confirmed the existence of the EI state through analyzing the condition for the divergence of the static excitonic susceptibility function. The numerical results have affirmed that both the electron-phonon coupling and the Coulomb attraction play an important role in establishing the excitonic condensed phase at low temperature. Most noteworthy, we have established phase diagrams of the excitonic condensate state in the system in the (U, g) plane including the BCS-BEC crossover. Phase diagrams have shown that at low temperature, the EI phase is only formed within a finite value range of the Coulomb attraction. The phase structure of the excitonic condensation in the system changes from the BCS-type which is similar to the condensation of Cooper pairs in superconductivity at small the Coulomb attraction to the BEC-type of tightly bound excitons if the Coulomb attraction is sufficiently large. Depending on the electron-phonon coupling constant and the Coulomb attraction, the BCS-BEC crossover boundary of the excitonic condensation state has also been constructed. Growing the temperature, the excitonic condensate window is shrunk and both SM and SC regions are expanded. Considering more meticulously kinetic nature of the excitonic condensate state via calculating the optical conductivity in these materials would be our worthwhile investigations in the future.

ACKNOWLEDGMENT

This work is funded by Ministry of Education and Training, Vietnam, under grant number B2021-MDA-14.

REFERENCES

[1] S. A. Moskalenko and D. W. Snoke, *Bose-Einstein Condensation of Excitons and Biexcitons and Coherent Nonlinear Optics with Excitons*. Cambridge Univ. Press, Cambridge, 2000.
[2] N. F. Mott, *The transition to the metallic state*, *Philos. Mag.* **6** (1961) 287.
[3] R. Knox in *Solid State Physics*, F. Seitz and D. Turnbull, eds., (New York), p. Suppl. 5 p. 100, Academic Press, (1963).
[4] W. Kohn, *Metals and insulators*, in *Many Body Physics*, C. de Witt and R. Balian, eds., (New York), Gordon & Breach, (1968).
[5] P. Wachter, B. Bucher and J. Malar, *Possibility of a superfluid phase in a Bose condensed excitonic state*, *Phys. Rev. B* **69** (2004) 094502.
[6] B. Bucher, T. Park, J. D. Thompson and P. Wachter, *Thermodynamical signatures of an excitonic insulator*, *arXiv:0802.3354 [cond-mat.str-el]* (2008) .
[7] P. Wachter, *Exciton condensation and superfluidity in* $TmSe_{0.45}Te_{0.55}$, *Advances in Materials Physics and Chemistry* **8** (2018) 120.
[8] A. Kogar, M. S. Rak, S. Vig, A. A. Husain, F. Flicker, Y. I. Joe et al., *Signatures of exciton condensation in a transition metal dichalcogenide*, *Science* **358** (2017) 1314.
[9] T. I. Larkin, A. N. Yaresko, D. Propper, K. A. Kikoin, Y. F. Lu, T. Takayama et al., *Giant exciton Fano resonance in quasi-one-dimensional* Ta_2NiSe_5, *Phys. Rev. B* **95** (2017) 195144.
[10] Y. Lu, H. Kono, T. Larkin, A. Rost, T. Takayama, A. Boris et al., *Zero-gap semiconductor to excitonic insulator transition in* Ta_2NiSe_5, *Nature Communications* **8** (2017) 14408.
[11] A. Nakano, T. Hasegawa, S. Tamura, N. Katayama, S. Tsutsui and H. Sawa, *Antiferroelectric distortion with anomalous phonon softening in the excitonic insulator* Ta_2NiSe_5, *Phys. Rev. B* **98** (2018) 045139.

[12] T. I. Larkin, R. D. Dawson, M. Höppner, T. Takayama, M. Isobe, Y.-L. Mathis et al., *Infrared phonon spectra of quasi-one-dimensional Ta_2NiSe_5 and Ta_2NiS_5*, *Phys. Rev. B* **98** (2018) 125113.
[13] F. X. Bronold and H. Fehske, *Possibility of an excitonic insulator at the semiconductor-semimetal transition*, *Phys. Rev. B* **74** (2006) 165107.
[14] D. Ihle, M. Pfafferott, E. Burovski, F. X. Bronold and H. Fehske, *Bound state formation and nature of the excitonic insulator phase in the extended Falicov-Kimball model*, *Phys. Rev. B* **78** (2008) 193103.
[15] N. V. Phan, K. W. Becker and H. Fehske, *Spectral signatures of the BCS-BEC crossover in the excitonic insulator phase of the extended Falicov-Kimball model*, *Phys. Rev. B* **81** (2010) 205117.
[16] B. Zenker, D. Ihle, F. X. Bronold and H. Fehske, *Electron-hole pair condensation at the semimetal-semiconductor transition: A BCS-BEC crossover scenario*, *Phys. Rev. B* **85** (2012) 121102(R).
[17] Z. Wang, D. A. Rhodes, K. Watanabe, T. Taniguchi, J. C. Hone, J. Shan et al., *Evidence of high-temperature exciton condensation in two-dimensional atomic double layers*, *Nature* **574** (2019) 76.
[18] P. Wachter, *Exciton condensation in an intermediate valence compound: $TmSe_{0.45}Te_{0.55}$*, *Solid State Commun.* **118** (2001) 645.
[19] T.-H.-H. Do, D.-H. Bui and V.-N. Phan, *Phonon effects in the excitonic condensation induced in the extended falicov-kimball model*, *Europhysics Letters* **119** (2017) 47003.
[20] T.-H.-H. Do, H.-N. Nguyen and V.-N. Phan, *Thermal fluctuations in the phase structure of the excitonic insulator charge density wave state in the extended falicov–kimball model*, *J. Electron. Mater.* **48** (2019) 2677.
[21] K. Sugimoto, S. Nishimoto, T. Kaneko and Y. Ohta, *Strong coupling nature of the excitonic insulator state in Ta_2NiSe_5*, *Phys. Rev. Lett.* **120** (2018) 247602.
[22] J. Lee, C.-J. Kang, M. J. Eom, J. S. Kim, B. I. Min and H. W. Yeom, *Strong interband interaction in the excitonic insulator phase of Ta_2NiSe_5*, *Phys. Rev. B* **99** (2019) 075408.
[23] M. Holt, P. Zschack, H. Hong, M. Y. Chou and T. C. Chiang, *X-Ray studies of phonon softening in $TiSe_2$*, *Phys. Rev. Lett.* **86** (2001) 3799.
[24] F. Weber, S. Rosenkranz, J.-P. Castellan, R. Osborn, G. Karapetrov, R. Hott et al., *Electron-phonon coupling and the soft phonon mode in $TiSe_2$*, *Phys. Rev. Lett.* **107** (2011) 266401.
[25] K. Kim, H. Kim, J. Kim, C. Kwon, J. S. Kim and B. J. Kim, *Direct observation of excitonic instability in ta2nise5*, *Nat. Commun.* **12** (2021) 1969.
[26] T.-H.-H. Do, H.-N. Nguyen, T.-G. Nguyen and V.-N. Phan, *Temperature effects in excitonic condensation driven by the lattice distortion*, *Physica Status Solidi B* **253** (2016) 1210.
[27] Y.-S. Zhang, J. A. N. Bruin, Y. Matsumoto, M. Isobe and H. Takagi, *Thermal transport signatures of the excitonic transition and associated phonon softening in the layered chalcogenide ta_2nise_5*, *Phys. Rev. B* **104** (2021) L121201.
[28] B. Zenker, D. Ihle, F. X. Bronold and H. Fehske, *On the existence of the excitonic insulator phase in the extended Falicov-Kimball model: a SO(2)-invariant slave-boson approach*, *Phys. Rev. B* **81** (2010) 115122.
[29] N. V. Phan, H. Fehske and K. W. Becker, *Excitonic resonances in the 2D extended Falicov-Kimball model*, *Europhys. Lett.* **95** (2011) 17006.
[30] T. Kaneko, T. Toriyama, T. Konishi and Y. Ohta, *Orthorhombic-to-monoclinic phase transition of Ta_2NiSe_5 induced by the Bose-Einstein condensation of excitons*, *Phys. Rev. B* **87** (2013) 035121.
[31] K. Sugimoto, T. Kaneko, and Y. Ohta, *Microscopic quantum interference in excitonic condensation of Ta_2NiSe_5*, *Phys. Rev. B.* **93** (2016) 041105(R).
[32] P. Wachter and B. Bucher, *Exciton condensation and its influence on the specific heat*, *Physica B* **408** (2013) 51.
[33] B. Zenker, H. Fehske, H. Beck, C. Monney and A. R. Bishop, *Chiral charge order in $1T$-$TiSe_2$: Importance of lattice degrees of freedom*, *Phys. Rev. B* **88** (2013) 075138.